ELSEVIER

Biochimica et Biophysica Acta 1527 (2001) 20–30

BIOCHIMICA ET BIOPHYSICA ACTA
BBA

www.bba-direct.com

Diadenosine phosphates and *S*-adenosylmethionine: novel boron binding biomolecules detected by capillary electrophoresis

Nicholas V.C. Ralston, Curtiss D. Hunt *

United States Department of Agriculture[1,2], Agricultural Research Service, Grand Forks Human Nutrition Research Center, 2420 2nd Ave. N., PO Box 9034, Grand Forks, ND 58202-9034, USA

Received 14 November 2000; received in revised form 8 March 2001; accepted 8 March 2001

Abstract

There is evidence that boron has a physiological role in animals and humans, but the search for boron binding biomolecules has been difficult because useful radioactive boron isotopes do not exist. To overcome this limitation we used capillary electrophoresis to identify and quantify boron binding to biomolecules by detecting the negative charge boron imparts to ligands. The effect of molecular structure and proximal electronic charges of adenosine and molecules with adenosine moieties including *S*-adenosylmethionine (SAM) and diadenosine polyphosphates (Ap_nA) were compared. The boron affinity of the test species varied with the rank order SAM-$\cong Ap_6A \cong Ap_5A > Ap_4A > Ap_3A \cong NAD^+ > Ap_2A >$ NADH $\cong$ 5′ATP $>$ 5′ADP $>$ 5′AMP $>$ adenosine $>$ 3′AMP $\cong$ 2′AMP $\cong$ cAMP $\cong$ adenine. Test species with vicinal *cis*-diols bound boron; species without those moieties did not. Boron binding affinity increased when proximal cationic moieties were present. Anionic moieties remote from the *cis*-hydroxyl binding site also positively influenced boron binding affinity. In the Ap_nA species, cooperative complexing of boron between the terminal ribose moieties apparently occurred. In these species boron affinity greater than expected for two monocomplexes was observed and binding affinities increased as more phosphate groups (beyond three) were present separating the terminal moieties. Our results indicate that Ap_6A, Ap_5A, Ap_4A, Ap_3A, and SAM have higher affinities for boron than any other currently recognized boron ligand present in animal tissues including NAD^+.

Keywords: Boron; Nicotinamide adenine dinucleotide; Diadenosine polyphosphate; *S*-Adenosylmethionine; Capillary electrophoresis

1. Introduction

Boron is an essential element for plants [1,2] and physiologic boron concentrations are needed to support metabolic processes in animals [3–11]. Embryological development in fish [3] and frogs [4] does not proceed normally in the absence of extracellular boron and there is evidence that chicks [5], rats [6,7], pigs [8], and humans [9–12] require physiological amounts of boron to support normal biologic functions.

Boron is an integral component of certain natural antibiotics [13–15] and forms stable boroesters with plant biomolecules such as rhamnogalacturonan-II [16]. The role of boron in these molecules is essential; in its absence these molecules no longer perform their normal physiologic functions [13–16]. That so few biomolecules that require boron for metabolic activity have been identified probably reflects the unique nature of boron radiochemistry and biochemistry. With radioactive half-lives of less than 1 s, traceable boron isotopes cannot be used to label boron binding ligands. Without radioisotopes, detection and identification of boron dependent biomolecules with reversible physiologic interactions are predicted to be very difficult because boron is likely to be dissociated during isolation and purification. The discovery, purification, and identification of the currently recognized boron dependent biomolecules was achieved because the bound boron formed four coordinate covalent bonds with the ligand, creating a thermodynamically stable complex that is almost undissociable in water [17]. However, many boron interactions with biological ligands are rapidly reversible [18–20] and difficult to detect with current techniques.

* Corresponding author. Fax: +1-701-795-8230;
E-mail: chunt@gfhnrc.ars.usda.gov

[1] The US Department of Agriculture, Agricultural Research Service, Northern Plains Area, is an equal opportunity/affirmative action employer and all agency services are available without discrimination.

[2] Mention of a trademark or proprietary product does not constitute a guarantee or warranty of the product by the US Department of Agriculture and does not imply its approval to the exclusion of other products that may also be suitable.

0304-4165/01/$ – see front matter
PII: S0304-4165(01)00130-1

Biomolecules possessing vicinal *cis*-diols or proximal hydroxyls in the correct orientations form boroesters with association constants that vary from weak to highly stable [17,21,22]. With a pK_a in solution of 9.2, boron is predominantly in the uncharged, planar, trigonal boric acid form (H_3BO_3) at physiological pH. However, when boron forms covalent bonds with biological ligands, its pK_a is reduced to ≥ 6 [23], and the majority of the boron in ligand complexes are in the tetrahedral negatively charged borate ($H_4BO_4^-$) form while occupying the binding site [24,25]. Detecting and quantifying the formation of these boroesters requires sensitive instrumentation, especially if the association is weak.

Capillary electrophoresis (CE) is an exquisitely sensitive technique that is able to distinguish minute differences in mass or charge among molecular species. In CE, all ions are carried towards the anode at rates determined by their molecular charge and hydrodynamic diameter. Positively charged molecules pass through the capillary faster than neutral molecules while the migration times of negatively charged species increase in proportion to their anionic charge. CE is uniquely suited to assess the affinity of ligands for boron because the negative charge contributed to the ligand by borate while it is in residence retards molecular migration through the capillary [26–28]. The boron binding affinity of ligands can be compared by measuring the proportional increases in their relative migration times in the presence of boron at increasing concentrations.

The *cis*-diols on the ribose moiety of numerous nucleotides bind to boron [26,28] as well as immobilized boronates [29–31]. With a K_{eq} of 15 mM, nicotinamide adenosine dinucleotide (NAD^+) [32] has the highest boron binding affinity presently recognized among biomolecules naturally occurring in animals. Although NAD^+ and reduced nicotinamide adenosine dinucleotide (NADH) both possess two ribose moieties, boron binding to the ribose adjacent to the NAD^+ nicotinamide is thought to be accentuated because of the cationic charge present [32]. Structurally similar to NAD^+ and NADH, the diadenosine phosphates (Ap_nA) possess two adenosine moieties linked by 2–6 phosphates and also bind boron [33].

Present in all cells with active protein synthesis, Ap_nA molecules function as signal nucleotides associated with platelet aggregation and neuronal response. The Ap_nA are putative 'alarmones' which reportedly regulate cell proliferation, stress response, and DNA repair [34–36]. The potential physiologic effects of boron interactions with Ap_nA have not been examined; however, their similarities to NAD^+ and NADH suggest boron binding by these molecules may be significant. At physiologic pH, the adenine moieties of Ap_nA are driven together by hydrophobic forces and stack interfacially [37,38]. Stacking of the terminal adenine moieties brings their adjacent ribose moieties into close proximity, a phenomenon that may potentiate cooperative boron binding between the opposed riboses. If such dicomplex chelates form, boron binding with diadenosine nucleotides may have higher binding affinities than monoadenosine nucleotides. Therefore, the effects of boron on the migration of the five naturally occurring forms of Ap_nA in which the ribose moieties are separated by 2–6 phosphates were compared.

S-Adenosylmethionine (SAM) is the predominant methyl donor in biological methylations and is a versatile cofactor in a variety of physiologic processes [39,40]. It is formed when ATP donates its adenosyl group to the sulfur of methionine, resulting in a cationic sulfonium at the 5′-carbon of the ribose. The proximity of this cationic group may stabilize the negatively charged borate in its ribose binding site. Furthermore the terminal cationic amine and free carboxylate on methionine may further stabilize boron in the SAM monocomplex.

The ribose present on adenosine and adenosine species phosphorylated on the 5′-carbon (adenosine 5′-monophosphate (5′AMP), adenosine 5′-diphosphate (5′ADP), adenosine 5′-triphosphate (5′ATP)) enable these species to bind boron; however, boron complexes with these monoadenosine species should be less stable than complexes of boron with SAM, Ap_nA or NAD^+ and NADH. Meanwhile the lack of ribose on adenine and the absence of an intact ribose binding site on adenosine species phosphorylated on the 2′- or 3′-carbon (adenosine 2′-monophosphate (2′AMP), adenosine 3′-monophosphate (3′AMP)) make these species suitable negative controls.

Boron interactivity with *cis*-diols has been exploited as a means of enhancing chromatographic separations in various methods including CE [26–28]. However, these interactions have not been utilized to find boron binding biomolecules. Therefore, we developed a CE method that used these interactions to detect boron binding by biological ligands that are structurally related (Fig. 1). To examine the influence of local charge on boron binding potential, the positive, neutral, or negative charge present on these molecules was exploited. The presence of one or two ribose moieties on these molecules was used to examine the characteristics of monocomplex boron binding and unimolecular dicomplex boron binding.

2. Materials and methods

2.1. Materials

Analytical grade adenine (ADN), adenosine (ADS), SAM, 2′AMP, 3′AMP, 5′AMP, 5′ADP, 5′ATP, diadenosine pyrophosphate (Ap_2A), diadenosine triphosphate (Ap_3A), diadenosine tetraphosphate (Ap_4A), periodate treated diadenosine tetraphosphate (Ap_4A-per), diadenosine pentaphosphate (Ap_5A), diadenosine hexaphosphate (Ap_6A), NAD^+, NADH, dimethylformamide (DMF), and analytical grade glycyl-glycine were purchased from Sigma

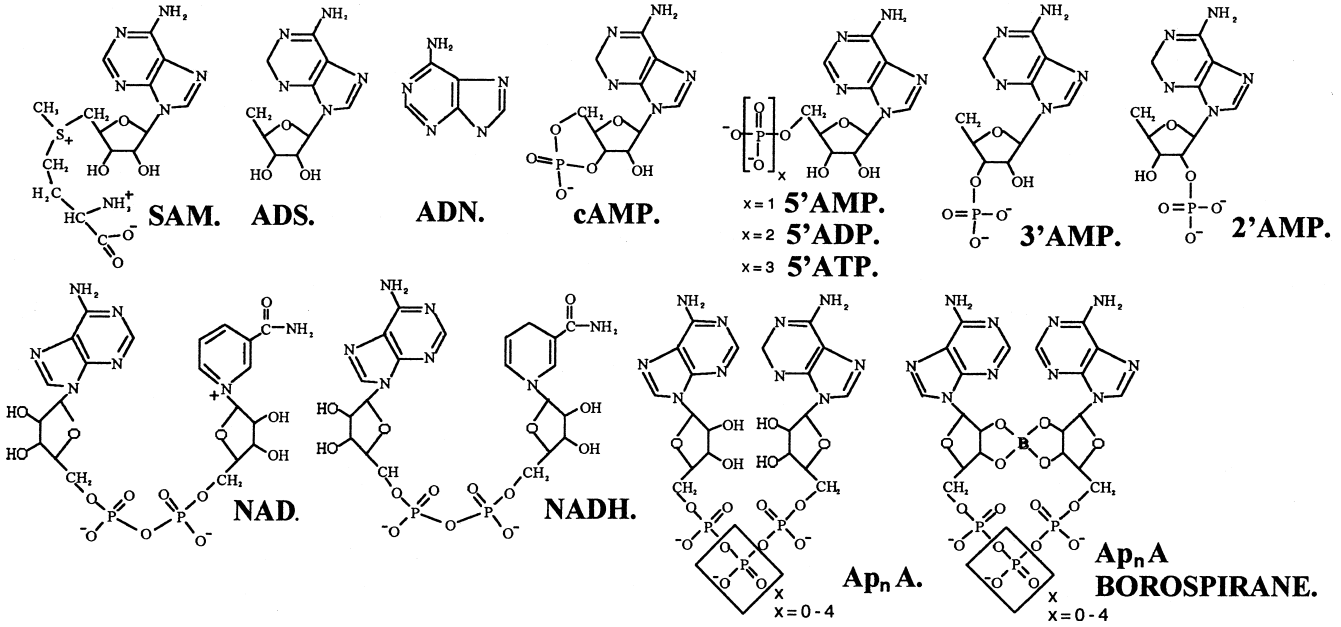

Fig. 1. Molecular structures of the test species.

Chemicals (St. Louis, MO). Ultra-pure *ortho*-boric acid was obtained from Johnson Matthey (Ward Hill, MA).

2.2. Preparation of samples and buffers

Stock samples of each analyte species were prepared at a concentration of 10 mM in 20 mM glycyl-glycine buffer and stored frozen until needed. Samples of these analyte species were either combined or individually diluted for use at a concentration of 1 mM. Boric acid prepared at 250 mM, and analytical grade glycyl-glycine prepared at 200 mM in 18 MΩ·cm water was adjusted to pH 8.4 with NaOH to attain equivalent final osmolarities. The glycyl-glycine buffer solution was passed through a 50 ml column of Amberlite (Sigma) to remove any contaminating boron. Analytical running buffers with boron concentrations 0.0, 0.1, 0.3, 1.0, 3.0, 10.0, and 30 mM were prepared by mixing graduated amounts of buffer and borate solutions.

2.3. Instrumentation

Capillary electrophoresis instrumentation consisted of a Beckman MDQ system (Palo Alto, CA) equipped with a photodiode array detector. The system was controlled by P/ACE System MDQ software. The uncoated fused silica CE columns (50 μm i.d., 375 μm o.d., 50 cm length to the detector, total length 60 cm; total volume in the capillary 1178 nl; volume to the window, 982 nl; Polymicro Technologies, Phoenix, AZ) were housed in a cartridge with a detection window of 100×800 μm. The capillary was conditioned prior to its first use by rinsing with 0.1 M NaOH for 20 min, then with 18 MΩ·cm water for 5 min.

2.4. Chromatography of analyte species

Analysis samples were diluted in 20 mM glycyl-glycine buffer solutions and run either alone or together with other experimental species along with DMF as a marker standard for comparison of the effects of various concentrations of boron in the running buffer. Analyte migrations in buffer solutions containing no boron were run before and after each boron concentration series. Running buffers (1.0 ml) in the cathode and anode vials were applied for analysis of migration times at each boron concentration examined. Sample solutions (1.0 mM) of each experimental species were prepared in 20 mM glycine buffer. Related monoadenosine species lacking one or the other of the *cis*-hydroxyls served as negative controls (Fig. 1). The negative control for diadenosine species was periodate treated Ap_4A (Ap_4A-P) in which the hydroxyls remain intact and available but their *cis* configuration has been disrupted (Fig. 1).

Samples of test species were injected into the capillary by applying positive pressure at 5 psi to the sample for 5 s, thus introducing a calculated 5.5 nl sample that contained approx. 5.5 pmole of test species in each analysis run. Sample separation by capillary electrophoresis was run for 15 min at 25 kV. The migration times of the species were determined by diode array monitoring total UV absorption in the range of 230–270 nm. The effect of boron on the migration time of each molecular species was tested individually and was observed to be identical to the effect observed when multiple species were tested in a single sample. Analyses of test species migration times were performed in separate experiments and the observed migration times were averaged to calculate the reported values.

Table 1
Relative migration times[a] of test species during capillary electrophoresis

	Monoadenosine species				
	SAM	ADS	5′AMP	5′ADP	5′ATP
Charge	+0.8	neutral	−2	−3	−4
	0.929 ± 0.001[b]	1.015 ± 0.001	2.236 ± 0.134	2.924 ± 0.274	3.321 ± 0.371
n	7	7	7	7	7
	Dinucleotide species				
	NAD^+	NADH			
Charge	−1	−2			
	1.303 ± 0.017	1.783 ± 0.045			
n	10	10			
	Diadenosine species				
	Ap_2A	Ap_3A	Ap_4A	Ap_5A	Ap_6A
Charge	−2	−3	−4	−5	−6
	1.811 ± 0.048	2.283 ± 0.096	2.520 ± 0.125	2.630 ± 0.140	2.690 ± 0.148
n	10	10	10	10	10
	Control species				
	ADN	cAMP	2′AMP	3′AMP	Ap_4A-P
Charge	neutral	−1	−2	−2	−4
	1.035 ± 0.010	1.627 ± 0.048	2.424 ± 0.173	2.429 ± 0.167	3.006 ± 0.023
n	7	7	7	7	4

[a]The migration times of these test species were divided by the migration time of the neutral standard DMF to yield the relative migration time ($\Delta\mu T$) for the species.
[b]Data shown are means ± S.D. of '*n*' independent analytical determinations.

Each sample analysis run included DMF as the neutral standard that traversed the capillary at the electroosmotic front. Capillary surfaces were reequilibrated between runs with a rinse (0.5 min, all rinses at 20 psi) of 0.1 M NaOH followed by a rinse (0.5 min) with 18 MΩ·cm water and a final rinse (2 min) with the next running buffer to be used.

2.5. Calculations

The relative migration time (μT) of each analyte was calculated by dividing the migration time of the sample species by the migration time of the neutral standard. The change in relative migration time ($\Delta\mu T$) induced by boron in the running buffer was calculated by dividing μT in the presence of boron by the μT for that analyte without boron.

The percentage of ligand–boron complex formation (%L-B) was calculated by determining the unit charge effect observed for each species in the presence of boron:

$$(\Delta\mu T\ n)/[(\mu T \text{ species } n+1)/(\mu T\ n)] \quad (1)$$

One unit of negative charge (corresponding to 100% boron saturation) was assumed to be present in association with species *n* when the $\Delta\mu T$ for that species is equal to (μT species *n*+1)/(μT species *n*), e.g., when $\Delta\mu T$ 5′ADP = (μT 5′ATP)/(μT 5′ADP). The pK_a on the terminal amine of SAM is 9.27, thus at pH 8.4 a positive charge is present on 86.5% of SAM molecules. The calculations performed to determine boron binding by SAM account for this partial charge. The pK_a of the amine may shift while proximal to

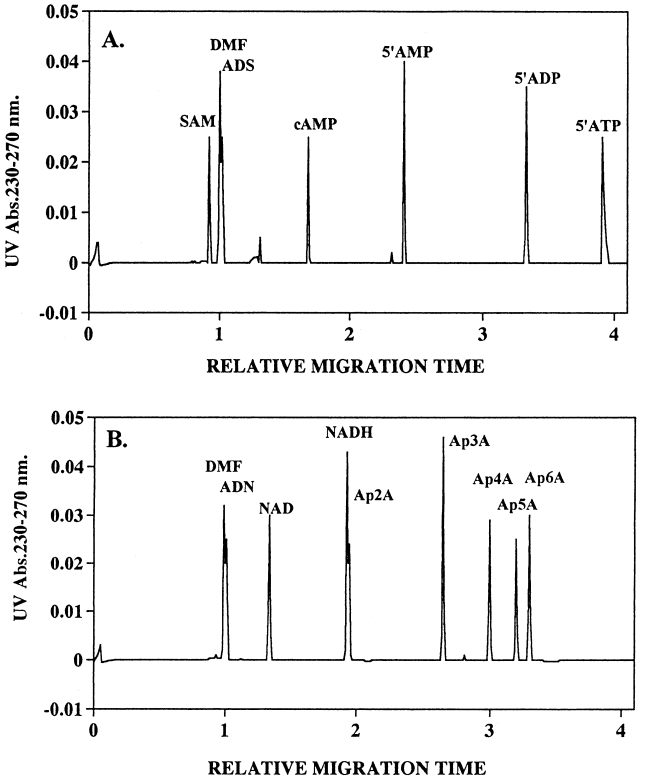

Fig. 2. High performance capillary electrophoresis separation of test species in borate free 200 mM glycyl-glycine buffer at pH 8.4. (A) Monoadenosines; (B) NAD^+/NADH, diadenosine polyphosphate species.

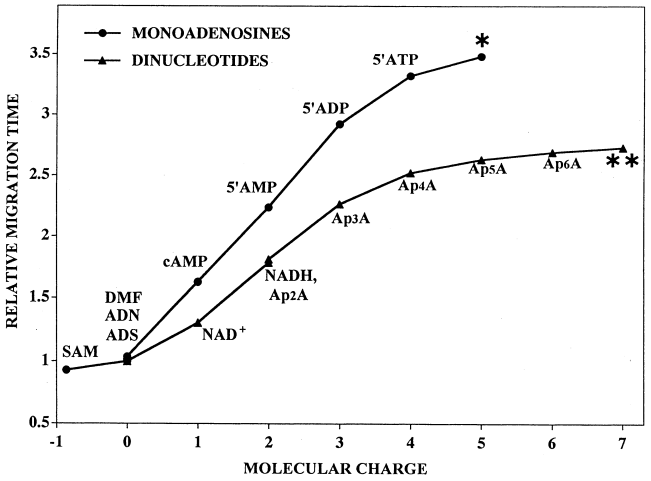

Fig. 3. Effect of molecular charge on migration time. The formal charges of the test species are plotted in relation to their migration time in capillary electrophoresis. The effect of charge on molecular μT follows the three parameter logistic model estimated using the nonlinear regression $y=\alpha/[1+\exp(\beta-\gamma x)]$. Regressions for monoadenosines and diadenosines were calculated independently for each data set. The asterisk denotes the mean value for the calculated μT of a monoadenosine species with five anionic charges: 4.642; the double asterisk denotes the mean value for the calculated μT of a diadenosine species with seven anionic charges: 3.315.

the anionic borate, but the magnitude of this effect was not examined.

The μT values of a monoadenosine with five anionic charges (μT species n+1 for ATP) and the μT of a diadenosine species with seven anionic charges (μT species n+1 for Ap_6A) were estimated by extrapolation of the equations that described the respective influences of charge on monoadenosine and diadenosine species. The migration of both classes of molecules followed similar three parameter logistic models for nonlinear regressions:

$$y = \alpha/[1+\exp(\beta-\gamma x)] \quad (2)$$

where α is the upper asymptote, and β and γ are first order rate constants.

Boron concentration at 100% saturation for each molecular species was calculated by applying the Michaelis-Menten model to plotting the relationship between % saturation and mM boron concentration or applying a linear model when that method yielded an improved correlation. K_{eq} was calculated as the boron concentration at 1/2 the saturation value.

3. Results

3.1. Migration behavior of test species

Migration times of each tested species run singularly did not change in the presence of other test species. Therefore, to directly compare sample migration times and the effect of boron on migration times, the test species were run in groups. Electropherograms of the UV absorption of the test species after separation by capillary electrophoresis in the absence of added boron are presented in Fig. 2.

3.2. Monoadenosine μT, $\Delta\mu T$, and %L-B

With a formal charge of +0.865 at pH 8.4, SAM migrated faster than the neutral standard and thus had a μT of less than one (Table 1, Figs. 2 and 3). Uncharged ADS and ADN migrated immediately after the neutral standard, with μT values only slightly greater than one. With a formal charge of -1, the μT of cAMP was intermediate between uncharged ADS and 5′AMP (formal

Table 2
Predicted change in migration time[a] ($\Delta\mu T$) with one additional unit of negative charge

SAM[b]	ADS	5′AMP	5′ADP	5′ATP[c]	NAD
1.151 ± 0.038	1.596 ± 0.045	1.298 ± 0.041	1.131 ± 0.020	1.048 ± 0.031	2.588 ± 0.078
NADH	Ap_2A	Ap_3A	Ap_4A	Ap_5A	Ap_6A[c]
1.637 ± 0.032	1.580 ± 0.024	1.184 ± 0.009	1.072 ± 0.004	1.037 ± 0.002	1.014 ± 0.002

[a]The change in molecular migration time predicted for each test species at boron saturation (when one additional unit of negative charge will have been acquired) is equal to (μT species n+1)/(μT species n), e.g., when $\Delta\mu T$ 5′ADP = (μT 5′ATP)/(μT 5′ADP). The data shown are means ± S.D. of n independent determinations (Table 1) individually applied to the data (Table 3) to yield the results in Table 4.

[b]The pK_a of the terminal amine of SAM is 9.27, thus at pH 8.4 there is a positive charge on 86.5% of the SAM molecules; the $\Delta\mu T$ for SAM at 100% boron saturation reflects this consideration.

[c]The $\Delta\mu T$ at 100% boron saturation for ATP and Ap_6A were calculated by applying the regression equation for each series and thereby extrapolating the μT of the next higher member in each series.

Table 3
Boron dependent change in relative migration times[a] ($\Delta\mu T$) of selected molecular species[b]

Boron (mM)	Monoadenosines				
	SAM	ADS	5′AMP	5′ADP	5′ATP
0.000	1.000 ± 0.000	1.000 ± 0.000	1.000 ± 0.000	1.000 ± 0.000	1.000 ± 0.000
0.100	1.002 ± 0.002	0.995 ± 0.007	1.000 ± 0.001	1.002 ± 0.004	1.004 ± 0.008
0.300	1.011 ± 0.003	0.996 ± 0.009	0.999 ± 0.001	1.003 ± 0.005	1.006 ± 0.010
1.000	1.039 ± 0.033	1.009 ± 0.022	1.007 ± 0.001	1.010 ± 0.007	1.014 ± 0.012
3.000	1.066 ± 0.032	1.029 ± 0.023	1.027 ± 0.003	1.019 ± 0.010	1.018 ± 0.014
10.000	1.190 ± 0.042	1.111 ± 0.007	1.086 ± 0.011	1.050 ± 0.022	1.033 ± 0.018
30.000	1.367 ± 0.029	1.255 ± 0.030	1.156 ± 0.029	1.104 ± 0.026	1.062 ± 0.020
	Dinucleotides				
	NAD^+	NADH			
0.000	1.000 ± 0.000	1.000 ± 0.000			
0.100	0.999 ± 0.022	1.004 ± 0.008			
0.300	1.029 ± 0.005	1.010 ± 0.007			
1.000	1.183 ± 0.035	1.021 ± 0.007			
3.000	1.404 ± 0.034	1.074 ± 0.016			
10.000	1.908 ± 0.049	1.207 ± 0.018			
30.000	2.612 ± 0.049	1.458 ± 0.027			
	Diadenosines				
	Ap_2A	Ap_3A	Ap_4A	Ap_5A	Ap_6A
0.000	1.000 ± 0.000	1.000 ± 0.000	1.000 ± 0.000	1.000 ± 0.000	1.000 ± 0.000
0.100	1.002 ± 0.002	1.000 ± 0.001	0.999 ± 0.001	0.999 ± 0.002	0.999 ± 0.002
0.300	1.007 ± 0.002	1.002 ± 0.000	1.001 ± 0.001	1.001 ± 0.001	1.000 ± 0.001
1.000	1.024 ± 0.002	1.008 ± 0.001	1.005 ± 0.001	1.003 ± 0.001	1.002 ± 0.001
3.000	1.073 ± 0.008	1.033 ± 0.023	1.016 ± 0.003	1.009 ± 0.004	1.006 ± 0.005
10.000	1.217 ± 0.012	1.083 ± 0.005	1.055 ± 0.003	1.036 ± 0.003	1.027 ± 0.004
30.000	1.499 ± 0.022	1.195 ± 0.038	1.126 ± 0.005	1.080 ± 0.004	1.062 ± 0.005
	Controls				
	ADN	cAMP	2′AMP	3′AMP	Ap_4A-P
0.000	1.000 ± 0.000	1.000 ± 0.000	1.000 ± 0.000	1.000 ± 0.000	1.000 ± 0.000
0.100	0.990 ± 0.013	0.996 ± 0.004	1.000 ± 0.002	1.000 ± 0.001	0.992 ± 0.000
0.300	0.988 ± 0.016	0.995 ± 0.005	1.000 ± 0.009	1.000 ± 0.000	0.992 ± 0.001
1.000	0.984 ± 0.019	0.992 ± 0.007	1.000 ± 0.003	1.000 ± 0.000	0.996 ± 0.003
3.000	0.987 ± 0.021	0.993 ± 0.008	1.000 ± 0.004	1.000 ± 0.000	0.998 ± 0.002
10.000	0.987 ± 0.025	0.989 ± 0.013	1.000 ± 0.005	0.999 ± 0.003	1.004 ± 0.004
30.000	0.990 ± 0.015	0.996 ± 0.005	1.000 ± 0.005	1.000 ± 0.003	1.004 ± 0.004

[a]Test species at 1.0 mM were electrophoretically separated at 28 kV in the capillary column in the presence of boron at the indicated concentrations.
[b]The change in relative migration time ($\Delta\mu T$) of each analyte was calculated by dividing the average migration time of the sample species by the migration time of the species in the boron buffer indicated by its relative migration time in the presence of 0 boron. Data shown are means ± S.D. from $n = 7$ independent analytical determinations for the monoadenosines, $n = 10$ for the diadenosines.

charge of −2). For 5′ADP and 5′ATP, each additional phosphate contributed a further unit of negative charge to the molecule that caused an incremental increase in migration times (Table 1 and Fig. 3).

Because hydrodynamic friction increases in proportion to species migration during electrophoresis, the $\Delta\mu T$ values predicted for test species possessing each additional unit of negative charge decreased in inverse proportion to their net anionic charges (Table 2). The migration times of the monoadenosine test species in relation to their formal charges followed the three parameter logistic model estimated by using the nonlinear regression equation $y = \alpha/[1+\exp(\beta-\gamma x)]$, where α is the upper asymptote and β and γ are first order rate constants. The predicted $\Delta\mu T$ value for 5′ATP with one additional negative charge was calculated by extrapolating the monoadenosine regression equation to include a species with five anionic charges. A monoadenosine with five anionic charges was predicted to have a μT of 3.417 (Table 2 and Fig. 3).

The rank order of boron dependent $\Delta\mu T$ among the monoadenosine species was SAM ≫ ADS > 5′AMP > 5′ADP > 5′ATP > 2′AMP ≅ 3′AMP ≅ cAMP ≅ ADN. When the $\Delta\mu T$ for these species (Table 3) was calculated relative to the predicted migration times at boron saturation (Table 2) the %L-B rank order was SAM ≫ 5′ATP > 5′ADP ≅ 5′AMP > ADS ≫ 2′AMP ≅ 3′AMP ≅ cAMP ≅ ADN (Table 4 and Fig. 4).

For SAM, increases in boron concentrations in the running buffers caused marked increases in the SAM μT (Table 3) consistent with a high boron binding affinity (Table

Table 4
Percent boron binding (%L-B) by mono- and dinucleotide ligands

Boron (mM)	Monoadenosines				
	SAM	ADS	5′AMP	5′ADP	5′ATP
0.0	0 ± 0%	0 ± 0%	0 ± 0%	0 ± 0%	0 ± 0%
0.1	2 ± 1%	−1 ± 1%	0 ± 0%	1 ± 3%	3 ± 11%
0.3	7 ± 2%	−0 ± 1%	0 ± 0%	2 ± 3%	3 ± 10%
1.0	28 ± 22%	3 ± 4%	2 ± 0%	6 ± 4%	16 ± 10%
3.0	46 ± 19%	6 ± 4%	6 ± 0%	13 ± 5%	22 ± 6%
10.0	128 ± 55%	19 ± 2%	20 ± 2%	36 ± 11%	47 ± 9%
30.0	237 ± 71%	42 ± 3%	51 ± 3%	75 ± 9%	96 ± 13%
	Dinucleotides				
	NAD^+	NADH			
0.0	0 ± 0%	0 ± 0%			
0.1	−0 ± 1%	1 ± 1%			
0.3	2 ± 0%	2 ± 1%			
1.0	11 ± 2%	3 ± 1%			
3.0	26 ± 3%	12 ± 3%			
10.0	58 ± 3%	33 ± 3%			
30.0	102 ± 4%	72 ± 2%			
	Diadenosines				
	Ap_2A	Ap_3A	Ap_4A	Ap_5A	Ap_6A
0.0	0 ± 0%	0 ± 0%	0 ± 0%	0 ± 0%	0 ± 0%
0.1	0 ± 0%	−0 ± 1%	−1 ± 2%	−3 ± 4%	−5 ± 7%
0.3	1 ± 0%	1 ± 0%	1 ± 1%	2 ± 4%	1 ± 6%
1.0	3 ± 0%	4 ± 0%	8 ± 1%	10 ± 4%	11 ± 6%
3.0	11 ± 2%	18 ± 11%	22 ± 5%	25 ± 14%	23 ± 26%
10.0	31 ± 2%	45 ± 2%	75 ± 7%	97 ± 17%	115 ± 30%
30.0	71 ± 1%	113 ± 4%	174 ± 13%	220 ± 27%	269 ± 42%

These test species were run at a 1 mM concentration in the capillary column in the presence of boron at the concentrations indicated. The accumulation of additional anionic charge originating from bound borate increased the relative migration times as detailed in Table 3. Dividing the values in Table 3 by the predicted change in migration time for each molecular species when one full unit of anionic charge was present ($\Delta\mu T$ at 100% boron saturation, Table 2), the % boron saturation (%L-B) of each molecular species was determined as indicated above.

4). Boron saturation occurred at approx. 7.0 mM boron (K_{eq} = 3.5 mM boron), and at still higher boron concentrations the electrophoretic migration of SAM was retarded further.

Boron binding by the other monoadenosine species was far less marked. Polyborates form in solution at concentrations higher than 30 mM, thus boron binding studies cannot be studied above this limit. At 30 mM, the highest boron concentration tested, the %L-B for ADS, 5′AMP, 5′ADP, and 5′ATP were 42, 51, 77, and 96%, respectively; the saturating boron concentrations for these species were 69.9, 58.1, 46.6, and 31.6 mM. Thus their apparent K_{eq} values were 34.9, 29.0, 23.3, and 15.8 mM. Boron interaction with the negative controls, 2′AMP, 3′AMP, cAMP and ADN, was negligible at all concentrations and their %L-B was consistently near zero.

3.3. NAD^+ and NADH μT, $\Delta\mu T$, and %L-B

With two anionic phosphate charges and a single cationic charge on the nicotinamide moiety, NAD^+ has a net formal charge of −1 and a μT that is proportionally less than NADH with a formal charge of −2 (Table 1 and Figs. 2 and 3). The μT of NADH is very similar to that of Ap_2A, a molecule that has the same formal charge and a similar mass (see below).

The predicted changes in migration times with one additional unit of negative charge on NAD^+ and NADH are shown in Table 2. The $\Delta\mu T$ of NAD^+ in the presence of increasing boron concentrations was greater than the $\Delta\mu T$ for NADH throughout all boron concentrations measured (Table 3). At a NADH:boron ratio of 1:30 (1 mM NADH:30 mM boron), the NADH was ≥75% boron saturated, achieving 100% saturation at 52.8 mM boron, thus it has a calculated K_d of 26.4 mM. In comparison, the boron dependent change in migration times of NAD^+ indicates approx. 100% boron saturation in the presence of 28.8 mM boron for a calculated K_{eq} of 14.4 mM.

3.4. Diadenosine polyphosphates μT, $\Delta\mu T$, and %L-B

Similar to the monoadenosines, the μT of Ap_nA species were proportional to the anionic charges present on the molecule (Table 1 and Figs. 2 and 3). The formal charge present on Ap_2A is −2 and the incremental increases in the μT through the Ap_nA series reflects the progressive

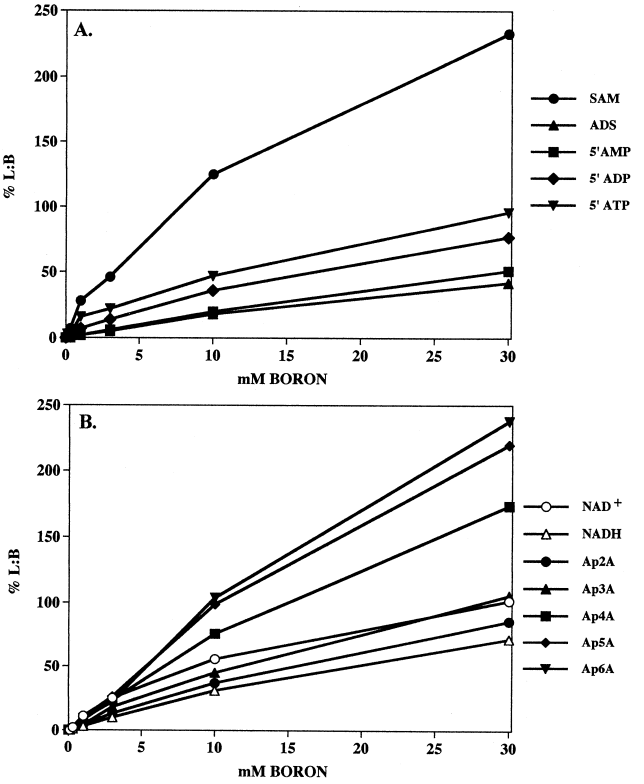

Fig. 4. Boron dependent unit charge effect on nucleotide migration in the presence of graduated boron concentrations. The unit charge contribution arising from boron complex formation $((\mu T\ n{+}1)-(\mu T\ n)/(\mu T\ n{+}1))$ in the presence of boron divided by μT in boron free buffer ($\Delta\mu T$) are shown for each test species. Depicted are the effects of boron on monoadenosine species (A), NAD^+, NADH, and the diadenosine polyphosphate species (B).

increases in anionic charge contributed by each additional phosphate. The predicted change in migration times with each additional unit of negative charge present in association with these species differed inversely to their net anionic charges as shown in Table 2. The migration times for all diadenosine phosphates increased as boron concentrations were increased in the running buffer (Table 3). Just as for the monoadenosines, the effect of charge on the μT of species in the dinucleotide series followed the nonlinear regression equation $y=\alpha/[1+\exp(\beta-\gamma x)]$. Because no diadenosines with seven phosphates (-7 formal charge) were available for assay, the value for the $\Delta\mu T$ of Ap_6A upon boron saturation was calculated using the predicted migration time for Ap_7A (2.760) extrapolated from the nonlinear logistic model for diadenosines (Fig. 3 and Table 2). Meanwhile, the μT of the negative control, periodate treated Ap_4A, was unaffected by the presence of boron in the running buffers (Table 3).

Boron binding was observed to progressively increase for Ap_2A through Ap_6A. Boron saturation for Ap_2A, Ap_3A, Ap_4A, Ap_5A, and Ap_6A occurred at 41.3, 26.0, 16.6, 13.0 and 10.8 mM respectively for calculated K_{eq} values of 20.6, 13.0, 8.3, 6.5, and 5.4 mM.

4. Discussion

4.1. Boroester detection by CE and mechanisms of boron binding

This work represents the first quantitative assay of boron binding by discrete molecular entities present in a panel of binding and non-binding biomolecules. Without radioactive boron isotopes to label boron binding biomolecules, these ligands and the complexes they form with boron have been difficult to detect and identify in biological samples. To overcome this limitation, a CE method was developed and used to examine the binding interaction between boron and various molecular species. Because the electrophoretic migration of a molecule is primarily determined by its electronic charge [41], formation of boroesters can be quantitatively detected by monitoring the influence of negatively charged borate on the migration of boron binding biomolecules in CE.

At physiological pH, $>98\%$ of boron in aqueous solution is in the uncharged and planar boric acid form (approx. 88% at pH 8.4). Boric acid acts as a Lewis acid, accepting hydroxyl oxygens and thus leaving an excess of protons. Boron binding is initiated when a hydroxyl oxygen present on the ligand releases its proton and approaches a planar boric acid to acquire its available pair of dative electrons and form a covalent bond. The complexed boron becomes a negatively charged tetrahedral borate. The tetrahedral borate can subsequently release the ester oxygen forming the link with the ligand or one of its hydroxyl oxygens. If a hydroxyl is released, the boron assumes the neutral and planar boric acid form once more and is available for the approach of another ligand hydroxyl to form a second boroester linkage [21]. A boron bound to a ligand through two covalent bonds is termed a monocomplex. When additional proximal hydroxyls with proper orientation are present, this process can be repeated until up to four boroester linkages with the ligand have formed and the assemblage is termed a dicomplex. Although these bonds are all reversible, borate in a dicomplex is thermodynamically stabilized in the binding site by the proximity of adjacent hydroxyls available for binding [42]. The stability of borate with the complex is therefore proportional to the number of ligand hydroxyls available for forming boroesters.

A molecular motif comprised of two or more cyclic structures that share a single nucleus is termed a 'spirane'. When borate binds the 2′- and 3′-hydroxyls on separate riboses, it forms a central point that participates in two five membered rings (-O-C-C-O-[B)-O-C-C-O-] and is termed a 'borospirane'. Boron in a dicomplex of four covalent bond associations with the ligand in a unimolecular borospirane motif has a much higher binding constant than boron in two separate monocomplexes, each interacting through two covalent bonds [25,42].

Because the pK_a of the boroester complex is approx. 6

[21], boron is predominantly (>98%) in the anionic form while it occupies a binding site, and indicates its presence by retarding ligand migration in CE. However, bound boron in the uncharged intermediate form does not retard ligand migration, although it is still present in the binding site. Therefore, CE may slightly underestimate boron binding to the extent that bound boron is present in the uncharged intermediate boric state instead of as anionic borate. Because this limitation is shared by all methods that employ electrostatics, the results obtained by CE are comparable to other means of measuring boron binding such as pH monitoring. However, the present method is more broadly applicable to analysis of biological samples than other methods because CE measures boron binding by each ligand and potential ligand independently.

Boron interactions with the nucleotide species examined in this study appear to be exclusively through the *cis*-hydroxyls of the ribose moieties because only molecules with both hydroxyls available exhibited increased migration times in the presence of boron. Because ADN migration was unaffected by even high concentrations of boron in the running buffers, it is clear the adenine moiety of the various species tested does not contribute to the observed boron interaction. There were no boron dependent increases in μT of cAMP, 2′AMP, or 3′AMP, because either the 2′- or the 3′-hydroxyl of ribose was already occupied by a phosphoester in these species. The importance of the adjacent *cis*-hydroxyl configuration is readily apparent when examining Ap_4A-P migration in the presence of boron (Table 3). Periodate cleaves between the carbons of vicinal *cis*-hydroxyls, thus disrupting the *cis* configuration of the ribose binding sites while leaving the hydroxyls of the 2′- and 3′-carbons intact. Without the *cis* configuration, these uncoordinated hydroxyl residues do not bind boron to a measurable extent.

Buffer selection is an important consideration when performing boron binding studies. Tricine has been used in previous capillary electrophoresis studies where boron was applied to selectively separate *cis*-diol molecular species from species that would otherwise comigrate [26]. However, the multiple hydroxyls in the molecular structure of tricine makes it highly interactive with boron. When equimolar pH 8.4 solutions of boron and tricine are mixed, a large pH shift is observed (data not shown), demonstrating that a tricine-borate complex has formed. On the other hand, the glycyl-glycine buffer used in these studies does not have proximal hydroxyl groups and did not show a pH shift upon mixing with boron solutions.

4.2. Boron and local electrostatic charges

Boron binding by SAM was far greater than by other monoadenosine species tested. This indicates that boron binding by the 2′-3′-*cis*-diols of the ribose moiety of SAM was electrostatically stabilized by the cationic sulfur of the methionine and interaction with the terminal amino and carboxyl groups on its methionine. The stabilizing effect of proximal cationic moieties on boroester stability was also evident when the migratory behaviors of NAD^+ and NADH were compared in the presence of boron. The anionic borate complex was electrostatically stabilized by the cationic nitrogen of the nicotinamide of NAD^+ (K_{eq} 14.4 mM), a charge that was not present on NADH (K_{eq} 26.4 mM). These data agree with observations reported earlier [32] where an indirect method of measuring boron binding was used to determine boron complex formation. In that study the binding constant for boron–NAD^+ was reported to be 15 mM, a value in excellent agreement with our observations.

4.3. Additive vs. cooperative boron binding by proximal intramolecular ribose moieties

NAD^+, NADH, and the Ap_nA species all possess a pair of ribose moieties held in close proximity, joined by 2–6 phosphodiesters. The higher boron affinity by the dinucleotide species is partially due to the additive effects of independent monocomplex binding by the two riboses present on NAD^+, NADH, and Ap_nA species. Because Ap_nA species are essentially two monoadenosine molecules joined through intervening phosphates, boron interaction with these two ribose moieties that is additive should be reflected by boron binding that is approximately twice that of the monoadenosines. Thus our data suggest that boron binding by NAD^+, NADH, Ap_2A, and Ap_3A is primarily additive because their %L-B at the various boron concentrations are not greater than twice that of the monoadenosines.

Boron binding by the ribose pair present on NADH, e.g. 31 %L-B at 1:10, was less than would be expected by additive effects of two monoadenosine riboses and is actually equivalent to the binding by 5′ADP. This suggests the neutral nicotinamide ribose has low boron affinity and the observed boron binding was primarily to the adenosine ribose. The increased boron binding by NAD^+ (56 %L-B at 1:10), is evidence of the effect of the cationic charge on the nicotinamide nitrogen on boron binding by its associated ribose. However, the observed binding does not exceed that expected for two independent monoadenosine ribose moieties, thus there apparently is no cooperative boron binding between the riboses of NAD^+.

The %L-B for Ap_2A and Ap_3A also indicate simple additive boron binding occurring through two independent monocomplexes. However, for Ap_nA with four or more intervening phosphates, boron binding apparently is cooperative, i.e., unimolecular dicomplex binding of boron occurs between the vicinal *cis*-hydroxyls of the opposing ribose moieties. Boron binding by Ap_4A, Ap_5A and Ap_6A appears enhanced, perhaps because formation of a boron dicomplex between ribose moieties of these species is more favorable. Computer modeling studies (data not shown) indicate that riboses separated by 2–3

phosphates cannot form an opposed dicomplex conformation with sufficient space for borate. However, members of the Ap_nA family with four or more phosphates can stabilize bound boron through cooperative chelation in a dicomplex borospirane.

4.4. Hydrodynamics and base stacking effects

The effects of hydrodynamic diameter on molecular migration were apparent in several aspects of this study. For instance, with a smaller hydrodynamic diameter and thus reduced frictional drag, the effect of added anionic charge on monoadenosine μT was proportionately greater than for the diadenosine species, which resulted in the higher rate constant and higher maximal relative migration observed for the monoadenosines. Similarly, the influence of boron binding on the hydrodynamic diameter of the molecule may have effects on molecular migration that deserve consideration.

Proton magnetic resonance spectroscopy of Ap_nA performed by Mayo and colleagues [37] indicates that adenine stacking in Ap_2A was close to 100% while adenine stacking in higher *n* members of the Ap_nA family progressively decreased towards a plateau value of approx. 50%. Our computer modeling studies of the Ap_nA species (data not shown) indicate that stacked adenine conformations prevent proper coordination of the ribose moieties with boron. This finding explains why boron binding by Ap_2A and Ap_3A is additive instead of cooperative. Because the stacked configuration is less prevalent in the higher order members of the Ap_nA family, the proximal riboses of these species are increasingly available for dicomplex borospirane formation. The borospirane dicomplex between riboses disturbs the stacked conformation and increases the hydrodynamic diameter of the molecules. This increase in hydrodynamic diameter will increase the frictional drag on the molecule, diminishing the migration retardation effect. When this occurs, the increase in migration time caused by the anionic charge of borate in the dicomplex would be diminished. Thus boron binding by these molecules may actually be much greater than our data indicate.

The base stacking behavior characteristic of Ap_nA molecules may also occur in NAD^+ and NADH because the relative migration times of NAD^+, NADH, and the Ap_nA species follow a uniform trend line relative to their formal molecular charge (see Fig. 2). Furthermore, the migration times of Ap_2A and NADH are very similar. If NADH was in the extended molecular conformation instead of stacked, the difference between its hydrodynamic diameter and that of Ap_2A should cause greater differences in their migration times.

4.5. Summary

The search for the precise physiologic functions of boron requires detection, identification, and determination of the relative affinities of boron ligands present in samples of biological origin. To meet these objectives, we developed a new CE method to detect and quantify boron binding by biological ligands naturally present in animal cells. We established that the SAM and Ap_nA families of biomolecules are boron ligands. Although the physiological consequences of boron binding with these molecular species remain unexplored, these novel ligands bind boron with higher affinities than NAD^+, formerly recognized as the highest affinity boron ligand present in animals. Our findings indicate that bound boron is stabilized in *cis*-diol binding sites by proximal cationic residues such as those present in SAM and NAD^+. Furthermore, ligands capable of forming boron dicomplexes between cooperating unimolecular *cis*-diol binding sites such as Ap_4A, Ap_5A, and Ap_6A have higher boron affinities than monocomplex ligands. Thus we suggest biomolecules with cationic residues proximal to borospirane binding sites would be expected to have even higher boron affinities than the species tested in the current study. Our new CE technique will be used to find other novel high affinity boron ligands among candidates isolated from biological samples.

Acknowledgements

This work was supported in part by a trust fund cooperative research agreement with US Borax.

References

[1] K. Warington, The effect of boric acid and borax on the broad bean and certain other plants, Ann. Bot. 37 (1923) 629–672.
[2] C.J. Lovatt, Evolution of xylem resulted in a requirement for boron in the apical meristems of vascular plants, New Phytol. 99 (1985) 509–522.
[3] R.I. Rowe, C.D. Eckert, Boron is required for zebrafish embryogenesis, J. Exp. Biol. 202 (1999) 1649–1654.
[4] D.J. Fort, E.L. Stover, P.L. Strong, F.J. Murray, C.L. Keen, Chronic feeding of a low boron diet affects reproduction and development in *Xenopus laevis*, Biol. Trace Elem. Res. 129 (1999) 2055–2060.
[5] C.D. Hunt, J.L. Herbel, J.P. Idso, Dietary boron modifies the effects of vitamin D3 nutriture on indices of energy substrate utilization and mineral metabolism, J. Bone Res. 9 (1994) 171–181.
[6] C.D. Hunt, J.P. Idso, Dietary boron as a physiological regulator of the normal inflammatory response: a review and current research progress, J. Trace Elem. Exp. Med. 12 (1999) 221–233.
[7] C.D. Hunt, Regulation of enzymatic activity: one possible role of boron in higher animals and humans, Biol. Trace Elem. Res. 66 (1998) 205–225.
[8] T.A. Armstrong, J.W. Spears, T.D. Crenshaw, F.H. Nielsen, Boron supplementation of a semipurified diet for weanling pigs improves feed efficiency and bone strength characteristics and alters plasma lipid metabolites, J. Nutr. 139 (2000) 2575–2581.
[9] C.D. Hunt, J.L. Herbel, F.H. Nielsen, Metabolic response of postmenopausal women to supplemental dietary boron and aluminum during usual and low magnesium intake: boron, calcium and magnesium absorption and retention and blood mineral concentrations, Am. J. Clin. Nutr. 65 (1997) 803–813.

[10] C.D. Hunt, B.J. Stoecker, Deliberations and evaluations of the approaches, endpoints, and paradigms for boron, chromium, and fluoride dietary recommendations, J. Nutr. 126 (1996) 2441–2451.
[11] F.H. Nielsen, S.K. Gallagher, L.K. Johnson, E.J. Nielsen, Boron enhances and mimics the same effects of estrogen therapy in postmenopausal women, J. Trace Elem. Exp. Med. 5 (1992) 237–242.
[12] R.L. Travers, G.C. Rennie, R.E. Newnham, Boron and arthritis: the results of a double-blind pilot study, J. Nutr. Med. 1 (1990) 127–132.
[13] K. Sato, T. Okazaki, K. Maeda, Y. Okami, New antibiotics, aplasmomycins B and C, J. Antibiot. 31 (1978) 632–634.
[14] D. Schummer, H. Irschik, H. Reichenbach, G. Hofle, Antibiotics from gliding bacteria, LVII. Tartrolons: new boron-containing macrodiolides from *Sorangium cellulosum*, Liebigs Ann. Chem. 1994 (1994) 283–289.
[15] J.D. Dunitz, D.M. Hawley, D. Miklos, D.N.J. White, Y. Berlin, R. Marusic, V. Prelog, Structure of boromycin, Helv. Chim. Acta 54 (1971) 1709–1713.
[16] M.A. O'Neill, D. Warrenfeltz, K. Kates, P. Pellerin, T. Doco, A.G. Darvill, P. Albersheim, Rhamnogalacturonan II, a pectic polysaccharide in the walls of growing plant cells, forms a dimer that is covalently cross-linked by a borate ester, J. Biol. Chem. 271 (1996) 22923–22930.
[17] M. Thellier, Y. Duval, M. Demarty, Borate exchanges of *Lemna minor* L. as studied with the help of the enriched stable isotopes and of a (n, alpha) nuclear reaction, Plant Physiol. 63 (1979) 283–288.
[18] C.J. Lovatt, W.M. Dugger, Boron, in: E. Frieden (Ed.), Biochemistry of Essential Ultratrace Elements, Plenum, New York, 1984, pp. 389–421.
[19] I.V. Berezin, K.H. Vill', K. Martinek, A.K. Yatsimirshii, Reversible inactivation of α-chymotrypsin resulting from interaction of Cu^{++} ions with the imidazole group of a histidine residue, Molekulyarnaya Biologiya 1 (1967) 719–728.
[20] G. Hausdorf, K. Kruger, G. Kuttner, H.-G. Holzhutter, C. Frommel, W.E. Hohne, Oxidation of a methionine residue in subtilisin-type proteinases by the hydrogen peroxide/borate system – an active site directed reaction, Biochim. Biophys. Acta 952 (1987) 1399–1400.
[21] M. Van Duin, J.A. Peters, A.P.G. Kieboom, H. Van Bekkum, I. Studies on borate esters, The pH dependence of the stability of esters of boric acid and borate in aqueous medium as studied by ^{11}B NMR, Tetrahedron 40 (1984) 2901–2911.
[22] W.D. Loomis, R.W. Durst, Chemistry and biology of boron, Biofactors 3 (1992) 229–239.
[23] J.A. Raven, Short- and long-distance transport of boric acid in plants, New Phytol. 84 (1980) 231–249.
[24] N.N. Greenwood, Boron, in: J.J. Bailar, H. Emeleus, R. Nyholm, A. Trotman-Dickerson (Eds.), Comprehensive Inorganic Chemistry, vol. 1, Pergamon, Oxford, 1973, pp. 665–990.
[25] U. Weser, Chemistry and structure of some borate polyol compounds of biochemical interest, in: C. Jorgensen, J. Neilands, R. Nyholm, D. Reinen, R. Williams (Eds.), Structure and Bonding, vol. 2, Springer-Verlag, New York, 1967, pp. 160–180.
[26] J.P. Landers, R.P. Oda, M.D. Schuchard, Separation of boron-complexed diol compounds using high performance capillary electrophoresis, Anal. Chem. 64 (1992) 2846–2851.
[27] S. Hoffstetter-Kuhn, A. Paulus, E. Gassmann, H.M. Widmer, Influence of borate complexation on the electrophoretic behavior of carbohydrates in capillary electrophoresis, Anal. Chem. 63 (1991) 1541–1547.
[28] J.P. Schaeper, S.S. Shamsi, N.D. Danielson, Separation of phosphorylated sugars using capillary electrophoresis with indirect photometric detection, J. Cap. Elec. 003:4 (1996) 215–221.
[29] G.D. Kuehn, J.H. Hageman, Boronic acid matrices for the affinity purification of glycoproteins and enzymes, in: A. Kenny, S. Fowell (Eds.), Practical Protein Chromatography Methods in Molecular Biology Series, vol. 11, Human Press, Totowa, NJ, 1992, pp. 45–71.
[30] R.R. Maestas, J.R. Prieto, G.D. Kuehn, J.H. Hageman, Polyacrylamine-boronate beads saturated with biomolecules: a new general support for affinity chromatography of enzymes, J. Chromatogr. 189 (1980) 225–231.
[31] J.H. Hageman, G.D. Kuehn, Assay of adenylate cyclase by use of polyacrylamide-boronate gel columns, Anal. Biochem. 80 (1977) 547–554.
[32] S.L. Johnson, K.W. Smith, The interaction of borate and sulfite with pyridine nucleotides, Biochemistry 15 (1976) 553–559.
[33] L.D. Barnes, A.K. Robinson, C.H. Mumford, P.N. Garrison, Assay of diadenosine tetraphosphate hydrolytic enzymes by boronate chromatography, Anal. Biochem. 144 (1985) 296–304.
[34] A.G. McLennan, Dinucleoside phosphates – an introduction, in: A.G. McLennan (Ed.), Ap_4A and Other Dinucleoside Polyphosphates, CRC Press, Boca Raton, FL, 1992, pp. 1–9.
[35] M.A. Gunther Sillero, J.C. Caeselle, Interactions of dinucleoside polyphosphates with enzymes and other proteins, in: A.G. McLennan (Ed.), Ap_4A and Other Dinucleoside Polyphosphates, CRC Press, Boca Raton, FL, 1992, pp. 205–229.
[36] A. Ogilvie, Extracellular functions for Ap_nA, in: A.G. McLennan (Ed.), Ap_4A and Other Dinucleoside Polyphosphates, CRC Press, Boca Raton, FL, 1992, pp. 229–275.
[37] K.H. Mayo, O.M. Mvele, R.N. Puri, Proton magnetic resonance spectroscopic analysis of diadenosine 5′,5‴-polyphosphates, FEBS Lett. 265 (1990) 97–100.
[38] N.H. Kolodny, L.J. Collins, Proton and phosphorus-31 NMR study of the dependence of diadenosine tetraphosphate conformation on metal ions, J. Biol. Chem. 261 (1986) 14571–14577.
[39] J.W. Kozarich, S-Adenosylmethionine-dependent enzyme activation, Biofactors 1 (1988) 123–128.
[40] H.A. Friedel, K.L. Goa, P. Benfield, S-Adenosyl-L-methionine. A review of its pharmacological properties and therapeutic potential in liver dysfunction and affective disorders in relation to its physiological role in cell metabolism, Drugs 38 (1989) 389–416.
[41] R.P. Oda, J.P. Landers, Introduction to capillary electrophoresis, in: J.P. Landers (Ed.), Handbook of Capillary Electrophoresis, CRC Press, Boca Raton, FL, 1997, pp. 1–47.
[42] C.A. Zittle, Reaction of borate with substances of biological interest, in: F. Ford (Ed.), Advances in Enzymology, vol. 12, Interscience Publishers, New York, 1951, pp. 493–527.